Adv. Appl. Prob. **36,** 616–642 (2004)
Printed in Northern Ireland

NUMERICAL INVERSION FOR LAPLACE TRANSFORMS OF FUNCTIONS WITH DISCONTINUITIES

T. SAKURAI,* *University of Melbourne*

Abstract

We analyse the role of Euler summation in a numerical inversion algorithm for Laplace transforms due to Abate and Whitt called the EULER algorithm. Euler summation is shown to accelerate convergence of a slowly converging truncated Fourier series; an explicit bound for the approximation error is derived that generalizes a result given by O'Cinneide. An enhanced inversion algorithm called EULER-GPS is developed using a new variant of Euler summation. The algorithm EULER-GPS makes it possible to accurately invert transforms of functions with discontinuities at arbitrary locations. The effectiveness of the algorithm is verified through numerical experiments. Besides numerical transform inversion, the enhanced algorithm is applicable to a wide range of other problems where the goal is to recover point values of a piecewise-smooth function from the Fourier series.

Keywords: Numerical transform inversion; Euler summation; Fourier series; Gibbs phenomenon; convergence acceleration; Laplace transform

2000 Mathematics Subject Classification: Primary 60-04
Secondary 60E10; 60K25; 65R10

1. Introduction

In probability models, it is often possible to obtain solutions to quantities of interest in terms of their Fourier, Laplace or Mellin transforms. This leaves the task of inverting the transform to obtain values of the inverse function. For transforms with suitable structure, the inverse function can be recovered by using tables of function–transform pairs. For more complicated transforms that are not given in these tables or cannot be easily expanded into a finite series of transforms that are, numerical transform inversion may be a viable option. In this paper, we analyse and extend a specific numerical Laplace-transform inversion algorithm developed by Abate and Whitt [1], called the EULER algorithm. One of the key features of the EULER algorithm, as the name suggests, is the use of a variant of Euler summation. Euler summation is a classical scheme for accelerating the convergence of certain sequences. In this paper, we give a detailed analysis of the crucial role played by Euler summation in EULER. Our analysis expands on a previous treatment by O'Cinneide [35]. It shows, for the first time, the improvement in the order of convergence afforded by Euler summation for inverse functions with discontinuities, possibly of infinite type, on a set of 'special' points. Further, we develop a new inversion algorithm based on EULER which works for inverse functions containing discontinuities at arbitrary locations. While our focus will be on inverting transforms of probability distribution

Received 9 July 2003; revision received 25 November 2003.
* Postal address: ARC Special Research Centre for Ultra-Broadband Information Networks, Department of Electrical and Electronic Engineering, University of Melbourne, Melbourne, VIC 3010, Australia.
Email address: t.sakurai@ee.mu.oz.au

and density functions occurring in stochastic models, the algorithms presented and analysed in this paper are applicable to a much broader range of functions and applications.

Many methods have been developed for performing numerical transform inversion. Davies [15, Chapter 19] gives a good summary of the more popular methods. While no method is universally superior, one that boasts a good combination of accuracy, robustness and simplicity and is well suited to probability applications is the Fourier-series method. The Fourier-series method is so-called because it involves approximating the inversion integral with an infinite Fourier series. The partial sums of a Fourier series thus formed are often slow to converge, so an effective convergence acceleration technique like Euler summation is invaluable.

Simon *et al.* [37] were the first to use Euler summation in the Fourier-series inversion algorithm. Since then, Hosono [28] and Abate and Whitt and their collaborators [1], [3], [11] have made refinements to the basic algorithm, and pioneered new areas of application. It appears that the algorithm EULER is now gaining widespread usage, with descriptions of it starting to appear in introductory applied probability texts such as [32], [36] and [38].

In the history of EULER and its predecessors, the theory has somewhat lagged behind the practice. Analysis of Euler summation in the Fourier-series method was commenced by Abate and Whitt [1], who gave an asymptotic justification of the benefit of Euler summation for the case of smooth inverse functions. However, it was not until O'Cinneide [35] that a clearer picture emerged as to why Euler summation should work. O'Cinneide recognized that the presence of a discontinuity at $t = 0$ in the inverse function is often the cause of slow convergence of the Fourier series. He gave two different arguments to show how Euler summation combats the Gibbs phenomenon associated with the discontinuity. Firstly, he derived a bound on the truncation error (reproduced below as Theorem 3.1) which showed that Euler summation substantially increases the order of convergence of the partial sums of the Fourier series. Secondly, he discovered that applying Euler summation is equivalent to multiplying the inverse function f by a trigonometric function g which is smooth at zero and at other 'special' points. The product function fg is smooth and so its Fourier series converges much more quickly than that of f. O'Cinneide called this effect *product smoothing*. In this paper, we derive a new bound on the truncation error which is consistent with the product-smoothing framework. Our result shows that Euler summation is effective for functions f that have discontinuities, possibly of infinite type, at $t = 0$ or at other special points. Our result can be regarded as unifying the two arguments presented by O'Cinneide.

When the inverse function has discontinuities (or other features exhibiting rapid variation) at locations other than $t = 0$ or other special points, EULER has difficulties. Indeed, it appears that all known numerical inversion methods have difficulties with such functions; relevant numerical evidence is presented in [1], [16], [18]. In their conclusion, Davies and Martin [16] remark that 'for functions with discontinuities, the use of a Fourier-series approach gives the greatest promise of accuracy'. In this paper, we show how the Fourier-series method can be made to realize this promise, by devising an algorithm that can cope with discontinuities at arbitrary locations. We call this algorithm EULER-GPS.

In terms of the types of inverse functions for which it is effective, EULER-GPS complements EULER and LATTICE-POISSON, another Fourier-series method due to Abate and Whitt [1], [3]. While EULER is suitable for smooth functions and LATTICE-POISSON works on the opposite extreme of lattice functions, EULER-GPS is good for piecewise-smooth functions.

The rest of this paper is organized as follows. In Section 2, we give a summary of the algorithm EULER. We provide an analysis of the effectiveness of Euler summation in EULER

in Section 3. In Section 4, we discuss other convergence acceleration methods that have been used in conjunction with the Fourier-series method. In Section 5, we present a new variant of Euler summation which forms the basis of EULER-GPS and, in Section 6, we present the algorithm EULER-GPS itself. We discuss parameter-selection strategies for EULER-GPS and give numerical examples. We close with some ideas for future work in Section 7.

2. The Fourier-series method and the algorithm EULER

In this section, we give a brief overview of the Fourier-series method of numerical transform inversion, focusing on the algorithm EULER. To be precise, we use the name EULER to refer to the one-dimensional Laplace-transform inversion algorithm described in detail by Abate *et al.* in Section 8.2.2 of [3], and summarized by O'Cinneide in [35]. This algorithm is the result of combining the algorithm of the same name from [1] with the rounding error control parameter l from [11]. Our description closely follows the treatment in [3].

Let g be a complex-valued function on $[0, \infty)$ with Laplace transform $\hat{g}$ given by

$$\hat{g}(s) = \int_0^\infty g(t)\mathrm{e}^{-st}\,\mathrm{d}t. \tag{2.1}$$

We form an exponentially damped version of g by setting

$$g_b(t) = \mathrm{e}^{-bt}g(t), \qquad b > 0, \tag{2.2}$$

and then construct the following function:

$$g_b^{[h]}(t) = \sum_{k=-\infty}^{\infty} g_b\left(t + \frac{2\pi k}{h}\right), \qquad h > 0. \tag{2.3}$$

We call $g_b^{[h]}$ the replication of g_b with period $2\pi/h$ (see [7, p. 193]). We see that $g_b^{[h]}$ is a superposition of translated copies of g_b, and that $g_b^{[h]}$ approximates g_b with increasing accuracy on the interval $[0, 2\pi/h)$ as the scaling parameter h is reduced. The replication device has a long history and its origin is difficult to trace. Some authors, such as Cooley *et al.* [12], refer to it as aliasing.

Loosely speaking, the replication function $g_b^{[h]}$ inherits the regularity of the original function g. For instance, if g has a jump discontinuity at $t = 0$, then more often than not, so too will $g_b^{[h]}$. We shall see later that lack of smoothness in $g_b^{[h]}$ represents the most significant challenge for the Fourier-series method of inversion. In probability applications, lack of smoothness at $t = 0$ is common; probability density functions or distribution functions of nonnegative random variables often have a jump discontinuity or some other kind of nonsmooth feature at the origin.

Since $g_b^{[h]}$ is periodic, it has an associated Fourier series. If we impose mild regularity conditions on $g_b^{[h]}$ at a point t, then the Fourier series converges to $g_b^{[h]}$ at t, and we may write

$$g_b^{[h]}(t) = \sum_{k=-\infty}^{\infty} c_k \mathrm{e}^{\mathrm{i}kht}, \tag{2.4}$$

where

$$\begin{aligned} c_k &= \frac{h}{2\pi}\int_0^{2\pi/h} g_b^{[h]}(t)\mathrm{e}^{-\mathrm{i}kht}\,\mathrm{d}t \\ &= \frac{h}{2\pi}\hat{g}(b + \mathrm{i}kh). \end{aligned} \tag{2.5}$$

Combining (2.3), (2.4) and (2.5) yields a variant of the Poisson summation formula:

$$\sum_{k=-\infty}^{\infty} g\left(t+\frac{2\pi k}{h}\right)\mathrm{e}^{-b(t+2\pi k/h)} = \frac{h}{2\pi}\sum_{k=-\infty}^{\infty}\hat{g}(b+\mathrm{i}kh)\mathrm{e}^{\mathrm{i}kht}. \tag{2.6}$$

We define $g^{[h]}(t)$ to be the expression on the right-hand side of (2.6) scaled by e^{bt}:

$$g^{[h]}(t) := \frac{h\mathrm{e}^{bt}}{2\pi}\sum_{k=-\infty}^{\infty}\hat{g}(b+\mathrm{i}kh)\mathrm{e}^{\mathrm{i}kht}. \tag{2.7}$$

The representation (2.7) is seen to be in the form of a Fourier series with the Fourier coefficients given by values of the Laplace transform. The basis of the Fourier-series method is to use $g^{[h]}(t)$ as an approximation to $g(t)$. The difference $e(t) = g^{[h]}(t) - g(t)$ is called the aliasing error and is found from the left-hand side of (2.6) to be given by

$$e(t) = \sum_{\substack{k=-\infty\\ k\neq 0}}^{\infty} g\left(t+\frac{2\pi k}{h}\right)\mathrm{e}^{-b(t+2\pi k/h)}. \tag{2.8}$$

The other sources of error associated with the Fourier-series method are truncation error and rounding error. Truncation error is the error incurred when the infinite sum in (2.7) is approximated by partial summation or a more sophisticated approximation technique such as Euler summation. Rounding error is the error incurred through the use of finite-precision arithmetic.

The Fourier-series method for Laplace-transform inversion is actually a collection of related algorithms based on the representation (2.7) and its variants (see [1] and Chapter 19 of [15] for summaries of some of the algorithms). The variant of (2.7) that underpins the algorithm EULER is derived by substituting

$$h = \frac{\pi}{lt} \tag{2.9}$$

and

$$b = \frac{A}{2lt} \tag{2.10}$$

in (2.7) for integer l and real A. The result is the representation

$$g^{[h]}(t) = \frac{\mathrm{e}^{A/2l}}{2lt}\sum_{k=-\infty}^{\infty}\hat{g}\left(\frac{A}{2lt}+\frac{\mathrm{i}k\pi}{lt}\right)\mathrm{e}^{\mathrm{i}k\pi/l}, \qquad t>0. \tag{2.11}$$

The values of A and l are chosen to simultaneously control the aliasing and rounding errors. The assignment (2.9) means that the period of replication is $2lt$. A typical choice is $l = 1$, which puts the inversion point t at the midpoint of the period. O'Cinneide [35] proved that the assignment (2.9) is crucial for maximizing the benefit of Euler summation. We shall explore this along with other aspects of the algorithm EULER in the next section.

As the final topic in this short overview of EULER, we review the definitions of the Euler transformation and the Euler summation. In the literature, there is both an Euler transformation for series (see [31] and [33, p. 144]) and an Euler transformation for sequences (see [33, p. 509] and [25, Chapter VIII]). If the sequence in question is the sequence of partial sums of the

series, then the two transformations are equivalent. In this paper, we will only refer to the Euler transformation for sequences. The Euler transformation (of order m) of a complex sequence $\{a_n\}$ is defined to be the sequence

$$b_n = \frac{1}{2^m} \sum_{j=0}^{m} \binom{m}{j} a_{n+j}. \tag{2.12}$$

The expression (2.12) is the classical Euler transformation proposed by Euler. The algorithm EULER uses a generalization of (2.12) which operates on every lth term of the sequence, starting with the nth term. This transformation applied to $\{a_n\}$ gives

$$b_n = \frac{1}{2^m} \sum_{j=0}^{m} \binom{m}{j} a_{n+jl}. \tag{2.13}$$

The generalization (2.13) was described in [11]; Boyd [5] employed the same transformation for application in a general Fourier-series context. Following O'Cinneide [35], we refer to (2.13) as the *Euler*(l, m) *transformation*. In the special case when the sequence $\{a_n\}$ consists of partial sums of a series, we call (2.13) *Euler*(l, m) *summation*. In EULER, Euler(l, m) summation is applied to partial sums of the infinite series in (2.11).

3. Effectiveness of Euler(l, m) summation

In this section, we give a theorem which helps to explain the excellent performance of Euler(l, m) summation in the algorithm EULER. Our theorem makes rigorous the product-smoothing framework discussed by O'Cinneide [35]. Like O'Cinneide, we state our results in the general context of Fourier series of certain piecewise-smooth functions.

Consider a 2π-periodic complex-valued function f on $\mathbb{R}$. Note that the $2\pi/h$-periodic function (2.3) of EULER can be transposed to the 2π-periodic framework via the scaling

$$f(t) := g_b^{[h]}(t/h). \tag{3.1}$$

We will assume that f has a Fourier-series expansion at t such that

$$f(t) = \sum_{k=-\infty}^{\infty} c_k \mathrm{e}^{\mathrm{i}kt},$$

where

$$c_k = \frac{1}{2\pi} \int_0^{2\pi} f(u) \mathrm{e}^{-\mathrm{i}ku}\, \mathrm{d}u.$$

Technical conditions for the convergence and equality of the Fourier-series expansion can be found in any standard reference on Fourier analysis, such as [8] or [41].

We are interested in the symmetric partial sums

$$S_n(t) = \sum_{k=-n}^{n} c_k \mathrm{e}^{\mathrm{i}kt}. \tag{3.2}$$

A well-known expression for the partial sums as a singular integral is

$$S_n(t) = \frac{1}{2\pi} \int_0^{2\pi} f(u+t) \frac{\sin(n+\frac{1}{2})u}{\sin u/2}\, \mathrm{d}u. \tag{3.3}$$

Following O'Cinneide, we define special argument values

$$t_{il} = \frac{(2i-1)\pi}{l}, \qquad i = 1, 2, \ldots, l. \tag{3.4}$$

In the algorithm EULER, the inversion point is transformed to lie at the point $t_{1l} = \pi/l$ (see Section 2), but in fact transformation to any one of the points t_{il} will work.

Euler(l, m) summation applied to a sequence of partial sums (3.2) at the argument values (3.4) is given by

$$E_n(l, m; t_{il}) := 2^{-m} \sum_{j=0}^{m} \binom{m}{j} S_{n+jl}(t_{il}). \tag{3.5}$$

A singular integral form for (3.5) is given by the following lemma.

Lemma 3.1. *The singular integral of the Euler(l, m) summation is*

$$E_n(l, m; t) = \frac{1}{2\pi} \int_0^{2\pi} f(u+t) \frac{\cos^m(lu/2) \sin(n + (1+lm)/2)u}{\sin u/2} \, \mathrm{d}u. \tag{3.6}$$

Proof. Combining (3.5) and (3.3) gives

$$\begin{aligned}
E_n(l, m; t) &= \frac{1}{2^m} \sum_{j=0}^{m} \binom{m}{j} \frac{1}{2\pi} \int_0^{2\pi} f(u+t) \frac{\sin(n + jl + \frac{1}{2})u}{\sin u/2} \, \mathrm{d}u \\
&= \frac{1}{2^{m+2} \mathrm{i}\pi} \sum_{j=0}^{m} \binom{m}{j} \int_0^{2\pi} \frac{f(u+t)}{\sin u/2} [\mathrm{e}^{\mathrm{i}u(n+jl+1/2)} - \mathrm{e}^{-\mathrm{i}u(n+jl+1/2)}] \, \mathrm{d}u \\
&= \frac{1}{2^{m+2} \mathrm{i}\pi} \int_0^{2\pi} \frac{f(u+t)}{\sin u/2} [\mathrm{e}^{\mathrm{i}u(n+1/2)}(1 + \mathrm{e}^{\mathrm{i}lu})^m - \mathrm{e}^{-\mathrm{i}u(n+1/2)}(1 + \mathrm{e}^{-\mathrm{i}lu})^m] \, \mathrm{d}u \\
&= \frac{1}{2^{m+2} \mathrm{i}\pi} \int_0^{2\pi} \frac{f(u+t)}{\sin u/2} [\mathrm{e}^{\mathrm{i}u(n+(1+ml)/2)}(\mathrm{e}^{\mathrm{i}lu/2} + \mathrm{e}^{-\mathrm{i}lu/2})^m \\
&\qquad\qquad - \mathrm{e}^{-\mathrm{i}u(n+(1+ml)/2)}(\mathrm{e}^{\mathrm{i}lu/2} + \mathrm{e}^{-\mathrm{i}lu/2})^m] \, \mathrm{d}u \\
&= \frac{1}{2\pi} \int_0^{2\pi} f(u+t) \frac{\cos^m(lu/2) \sin(n + (1+ml)/2)u}{\sin u/2} \, \mathrm{d}u.
\end{aligned}$$

The expression (3.6) will prove useful later when we derive bounds for the approximation error of Euler(l, m) summation.

The properties of important summation methods for Fourier series such as partial summation, Fejér summation and Poisson summation have been well studied; see, for example, [8]. To analyse summation methods, it is expedient to express the nth sum as a convolution integral of the form $(2\pi)^{-1} \int_0^{2\pi} f(u+t) k_n(u) \, \mathrm{d}u$, as we have done for ordinary partial summation (3.3) and Euler(l, m) summation (3.6). The quantity k_n is known as the *summability kernel* of the summation method. From (3.6), we see that the kernel associated with Euler(l, m) summation is

$$k_n(u) = \frac{\cos^m(lu/2) \sin(n + (1+lm)/2)u}{\sin u/2}. \tag{3.7}$$

Hardy [25, p. 364] briefly discussed the Euler kernel (for the case $n = 0$ and $l = 1$). He noted that the Euler kernel does not possess the convergence-inducing properties of some other

summation kernels, such as the Fejér and Poisson kernels. Consequently, with respect to *summability*, Euler(l, m) summation is not as powerful as these other methods. However, in relation to *approximation* at the special points t_{il}, we will see that Euler(l, m) summation can be remarkably effective provided that the approximated function has nice regularity properties.

We begin our analysis by reviewing the quality of the approximation of f by the partial sums S_n. It is well known that the order of convergence of S_n to f is related to the regularity of f (see [8, p. 105]). Stronger regularity—such as continuity of higher derivatives—translates to a higher order of convergence. In the most benign case of an analytic f, there is exponential convergence, namely

$$|f(t) - S_n(t)| \leq \beta^n$$

for some $\beta < 1$ (see [34, pp. 177–179]). To take another example, if f has a pth derivative of bounded variation and continuous lower derivatives, where $p \geq 1$, then we have arithmetic convergence with index p, namely

$$|f(t) - S_n(t)| \leq An^{-p}$$

for some constant A (see [29, p. 52]).

When f has a jump discontinuity, the partial sums exhibit spurious oscillations near the discontinuity that are symptomatic of the Gibbs phenomenon. For detailed descriptions of the Gibbs phenomenon see [26] or [9]. The maximum overshoot associated with the Gibbs phenomenon does not diminish as $n \to \infty$, so that

$$\max_{0 \leq t \leq 2\pi} |f(t) - S_n(t)| \sim O(1).$$

While the persistence of the overshoot is problematic, the most damaging consequence of a jump discontinuity from our perspective is retardation of the convergence of the Fourier series for points away from the discontinuity. The best order of convergence of the partial sums away from the discontinuity is only $O(1/n)$ (see [29]).

An order of convergence of $O(1/n)$ renders approximation by partial summation impractical if high accuracy is desired. Fortunately, the convergence can often be accelerated using an alternate method of summation such as Euler(l, m) summation.

Euler(l, m) summation belongs to the class of linear sequence transformations that are regular (see [25, p. 179]). To yield a computational advantage over partial summation, we also want Euler(l, m) summation to improve the order of convergence. If it does, then, to use the terminology of sequence transformations (see [40]), we say that Euler(l, m) summation is *accelerative*. O'Cinneide [35] proved that Euler(l, m) summation is accelerative for Fourier series evaluated at t_{il} for the class of functions that have $k + 1$ bounded, piecewise-continuous derivatives. Discontinuities in f or its derivatives are permitted only at $t = 0$. Denoting this class of functions by $\mathcal{BPC}^{k+1}$ and the kth derivative of f by $f^{(k)}$, we now state O'Cinneide's theorem. We use $\|\cdot\|_\infty$ to denote the supremum norm.

Theorem 3.1. (O'Cinneide [35].) *If $f \in \mathcal{BPC}^{k+1}$ and n is an integer multiple of l, then the approximation error incurred by $E_n(l, m; t_{il})$ satisfies the following bound:*

$$|E_n(l, m; t_{il}) - f(t_{il})| \leq \frac{l^{m+1}}{2^m \pi} \left(\sum_{\substack{j=1 \\ j \text{ odd}}}^{k-1} |\gamma_j(f)| \frac{(j+m)!}{j!\, n^{j+m+1}} \right) + \frac{4}{kn^k} \|f^{(k+1)}\|_\infty,$$

where $\gamma_j(f) := f^{(k)}(2\pi^-) - f^{(k)}(0^+)$.

Including the condition that n be an integer multiple of l corrects an omission in [35]. The condition is required in the proof of Theorem 1 of [35, p. 322] to ensure that terms with an odd power of $1/n$ vanish. Note that our parameter n—which is the same as that of O'Cinneide [35]—is related to the parameter of Abate *et al.* [3] by

$$n = n'l + l. \tag{3.8}$$

where n' denotes the parameter of Abate *et al.* (though they use the notation n). Hence, Abate *et al.* implicitly define n to be an integer multiple of l.

The piecewise continuity of the $(k+1)$th derivative can be relaxed to obtain related bounds for a larger space of functions (e.g. functions with Lebesgue integrable $(k+1)$th derivative), but here and in other results in this paper we restrict our attention to functions with a piecewise-continuous $(k+1)$th derivative to simplify statements.

Remark 3.1. We see from Theorem 3.1 that, if $k \leq m+2$, then

$$|E_n(l, m; t_{il}) - f(t_{il})| \sim O(n^{-k}) \quad \text{as } n \to \infty,$$

otherwise

$$|E_n(l, m; t_{il}) - f(t_{il})| \sim O(n^{-(m+2)}) \quad \text{as } n \to \infty.$$

Now we state a new result showing that Euler(l, m) summation is effective for a wider class of piecewise-smooth functions than that covered by Theorem 3.1. Our result shows that Euler(l, m) summation can overcome discontinuities at the special points

$$t'_{il} = \frac{2i\pi}{l}, \qquad i = 0, 1, 2, \ldots, l-1, \tag{3.9}$$

confirming O'Cinneide's remarks regarding the existence of a product-smoothing framework. The result applies to the space of functions that are absolutely integrable and have $k+1$ piecewise-continuous derivatives. Discontinuities in f or its derivatives—which may be of infinite type—are permitted only at the points t'_{il} given by (3.9). We shall denote this class of functions by $\mathcal{PC}_l^{k+1}$. We use the standard notation $\|\cdot\|_1$ for the L_1 norm.

Theorem 3.2. *If* $f \in \mathcal{PC}_l^{k+1}$ *and*

$$r := \min(k+1, m+1), \tag{3.10}$$

then the approximation error incurred by $E_n(l, m; t_{il})$ *satisfies the bound*

$$|E_n(l, m; t_{il}) - f(t_{il})| \leq \frac{2\|f_c^{(r)}\|_1}{\pi(r-1)(n + (m+1)l/2)^{r-1}},$$

where

$$f_c(u) := f(u + t_{il}) \cos^{m+1}\left(\frac{lu}{2}\right). \tag{3.11}$$

Proof. Define the first difference $\Delta E_n(l, m; t_{il})$ of the sequence $\{E_n(l, m; t_{il})\}$ to be

$$\Delta E_n(l, m; t_{il}) := E_n(l, m; t_{il}) - E_{n-1}(l, m; t_{il}).$$

From (3.6) we obtain that

$$\begin{aligned}\Delta E_n(l,m;t_{il}) &= \frac{1}{2\pi}\int_0^{2\pi} f(u+t_{il})\frac{\cos^m(lu/2)\sin(n+lm/2+1/2)u}{\sin u/2}\,\mathrm{d}u \\ &\quad - \frac{1}{2\pi}\int_0^{2\pi} f(u+t_{il})\frac{\cos^m(lu/2)\sin(n+lm/2-1/2)u}{\sin u/2}\,\mathrm{d}u \\ &= \frac{1}{\pi}\int_0^{2\pi} f(u+t_{il})\cos^m\left(\frac{lu}{2}\right)\cos\left(n+\frac{ml}{2}\right)u\,\mathrm{d}u. \end{aligned} \tag{3.12}$$

Define

$$\Delta\tilde{E}_n(l,m;t_{il}) := \Delta E_n(l,m;t_{il}) + \Delta E_{n+l}(l,m;t_{il}).$$

Using (3.12) we find that

$$\begin{aligned}&\Delta\tilde{E}_n(l,m;t_{il}) \\ &= \frac{1}{\pi}\int_0^{2\pi} f(u+t_{il})\cos^m\left(\frac{lu}{2}\right)\left\{\cos\left(n+\frac{ml}{2}\right)u+\cos\left(n+l+\frac{ml}{2}\right)u\right\}\mathrm{d}u \\ &= \frac{2}{\pi}\int_0^{2\pi} f(u+t_{il})\cos^{m+1}\left(\frac{lu}{2}\right)\cos\left(n+\frac{(m+1)l}{2}\right)u\,\mathrm{d}u \\ &= \frac{2}{\pi}\int_0^{2\pi} f_{\mathrm{c}}(u)\cos(n_1u)\,\mathrm{d}u, \end{aligned} \tag{3.13}$$

where $n_1 := n + (m+1)l/2$ and f_{c} is defined in (3.11). The aim is to obtain an asymptotic expansion in negative powers of n_1 by performing repeated integration by parts on (3.13). In this procedure, we differentiate f_{c} and integrate the cosine factor. The use of integration by parts to derive asymptotic expansions of integrals is a well-established technique: see Chapter 3 of [4].

For convenience, define $\chi(u) := \cos^{m+1}(lu/2)$. By definition, $f(u+t_{il})$ and its derivatives have possible discontinuities when $u + t_{il} = t'_{jl}$, for t'_{jl} defined by (3.9). In contrast, it can be easily verified that χ has zeros of order $m+1$ at $t'_{jl} - t_{il}$; in other words,

$$\chi^{(p)}(t'_{jl} - t_{il}) = 0 \quad \text{for } 0 \le p \le m.$$

We conclude therefore that $f_{\mathrm{c}} \in \mathrm{C}^{\gamma}$, where $\gamma = \min(k+1, m)$. The continuity of the first γ derivatives of f_{c} ensures that when we iteratively integrate (3.13) by parts r times (where r is given by (3.10)), all nonintegral terms vanish and we are left with

$$\Delta\tilde{E}_n(l,m;t_{il}) = (-1)^{\lfloor 3r/2\rfloor}\frac{2}{\pi n_1^r}\int_0^{2\pi} f_{\mathrm{c}}^{(r)}(u)\phi_r(n_1u)\,\mathrm{d}u, \tag{3.14}$$

where, by the Leibnitz rule for differentiation of a product,

$$f_{\mathrm{c}}^{(r)}(u) = \sum_{p=0}^{r}\binom{r}{p} f^{(r-p)}(u+t_{il})\chi^{(p)}(u) \tag{3.15}$$

and

$$\phi_r(u) = \begin{cases}\sin(u) & \text{if } r \text{ is odd,}\\ \cos(u) & \text{if } r \text{ is even,}\end{cases} \tag{3.16}$$

and where $\lfloor x \rfloor$ denotes the greatest integer less than or equal to x. The expression (3.14) relies on the integrability of f_c and, in the sequel, we will require absolute integrability. The absolute integrability of f_c can be confirmed from (3.15). The terms in the sum corresponding to $p = 0, 1, \ldots, r-1$ are assured to be continuous because, whenever $f^{(r-p)}$ has a (possibly infinite) discontinuity, $\chi^{(p)}$ has a zero. The $p = r$ term is also absolutely integrable because, by definition, f is absolutely integrable.

From (3.14) we obtain a bound for $|\Delta \tilde{E}_n(l, m; t_{il})|$:

$$|\Delta \tilde{E}_n(l, m; t_{il})| \leq \frac{2\|f_c^{(r)}\|_1}{\pi n_1^r}.$$

It remains to bound the approximation error:

$$\begin{aligned}
|E_n(l, m; t_{il}) - f(t_{il})| &\leq \sum_{j=n+1}^{\infty} |\Delta E_j(l, m; t_{il})| \\
&\leq \sum_{j=n+1}^{\infty} |\Delta \tilde{E}_j(l, m; t_{il})| \\
&\leq \frac{2\|f_c^{(r)}\|_1}{\pi} \sum_{j=n+1}^{\infty} \frac{1}{(j + (m+1)l/2)^r} \\
&\leq \frac{2\|f_c^{(r)}\|_1}{\pi} \int_n^{\infty} \frac{1}{(x + (m+1)l/2)^r} \, \mathrm{d}x \\
&= \frac{2\|f_c^{(r)}\|_1}{\pi(r-1)(n + (m+1)l/2)^{r-1}}.
\end{aligned}$$

This completes the proof.

We provide an intuitive explanation for the performance of Euler(l, m) summation. Consider the expression (3.7) for the kernel k_n of Euler(l, m) summation. The kernel attains a maximum of $2n + 1 + lm$ at 0, and has zeros of order m at the points $(2i - 1)\pi/l$ for $i = 1, 2, \ldots, l$. If we now consider the integrand of the singular integral of Euler(l, m) summation (3.6), we see that, when $k_n(u)$ is at its maximum value, $f(u + t_{il}) = f(t_{il})$ and, when k_n has a zero of order m, $f(u + t_{il}) = f(t'_{il})$. In other words, the Euler(l, m) summation kernel emphasizes the function value at the inversion point and suppresses the function value at the discontinuities with zeros of high order. Suppressing the discontinuities in this smooth fashion increases the rate of decay of the Fourier coefficients.

The theorem explains why the algorithm EULER works for functions that are unbounded at zero or have unbounded derivatives at zero [35]. An important case for applications is the gamma density function. See Section 6.1.4 for an example involving the inverse Gaussian density. Another example is the steady-state waiting-time distribution in the M/G/1 queue, which is known to have an atom at zero. Numerical investigations reveal that the atom has negligible effect on the accuracy (see the comment in the conclusion of [2]), and our result explains why.

Remark 3.2. The proof shows that evaluating $E_n(l, m; t)$ at $t = t_{il}$ gives the best order of approximation because, at these points, the zeros of χ coincide with the discontinuities of f.

If t differs from t_{il}, then, unlike (3.14), terms generated by integration by parts of order $O(n_1^{-j})$ for $j = 1, 2, \ldots, r-1$ will be present. As t approaches t_{il}, the nulling effect of χ will have an increasing influence and the magnitudes of these terms will decrease. Thus, there will be a kind of nonuniformity of convergence of $E_n(l, m; t)$ with respect to t. Boyd [5] illustrated the nonuniformity of convergence for the example of a sawtooth function.

Theorem 3.2 shows that, in theory, we can always make the approximation error as small as we like by choosing n large enough. However, to achieve a small bound on the approximation error for a *practical* value of n, we require that the numerator term $\|f_c^{(r)}\|_1$ is not large. Evidently, this condition holds for many probability functions since numerical studies point to a value of n of about 40 to be sufficient for good accuracy in many cases (see [3] and references therein).

From (3.15), we see that the size of $\|f_c^{(r)}\|_1$ will not be large if the first r derivatives of f do not have large magnitudes away from the special points given by (3.9). To see how the approximation error is related to the derivatives of the inverse function g, we now express the approximation error not in terms of f_c but in terms of a function more closely related to g. Using (2.3), (2.9) and (3.1), we can rewrite (3.13) as

$$\begin{aligned}\Delta\tilde{E}_n(l, m; t_{il}) &= \frac{2}{\pi}\int_0^{2\pi}\sum_{k=-\infty}^{\infty} g_b\left(\frac{u + t_{il} + 2\pi k}{h}\right)\cos^{m+1}\left(\frac{lu}{2}\right)\cos(n_1 u)\,\mathrm{d}u \\ &= \frac{2}{\pi}\int_{-t_{il}}^{\infty} g_b\left(\frac{u + t_{il}}{h}\right)\cos^{m+1}\left(\frac{lu}{2}\right)\cos(n_1 u)\,\mathrm{d}u \\ &= \frac{2}{\pi}\int_0^{\infty} g_b\left(\frac{u}{h}\right)\sin^{m+1}\left(\frac{lu}{2}\right)\cos(n_1(u - t_{il}))\,\mathrm{d}u.\end{aligned}$$

Define $w(u) := g_b(u/h)$ and $w_s(u) := w(u)\sin^{m+1}(lu/2)$. Clearly, w is simply a scaled version of g_b where the inversion point t is scaled to $u = \pi/l$. Repeated integration by parts yields that

$$\Delta\tilde{E}_n(l, m; t_{il}) = (-1)^{\lfloor 3r/2\rfloor}\frac{2}{\pi n_1^r}\int_0^{\infty} w_s^{(r)}(u)\phi_r(n_1(u - t_{il}))\,\mathrm{d}u,$$

where ϕ_r is given by (3.16). This expression is equivalent to (3.14). Thus, we see that the size of the approximation error is determined by the derivatives of w_s, where w_s is the inverse function altered by scaling, exponential damping and smoothing (by $\sin^{m+1}(lu/2)$). If $w_s^{(r)}$ does not have large magnitude, then the numerator term will not be large. Moreover, if the first r derivatives of g do not have large magnitudes away from the points $0, 2t, 4t, 6t, \ldots$, where t is the inversion point, then $w_s^{(r)}$ will not have large magnitude.

Theorem 3.2 shows that, for $k \le m$,

$$|E_n(l, m; t_{il}) - f(t_{il})| \sim O(n_1^{-k}) \quad \text{as } n \to \infty,$$

otherwise

$$|E_n(l, m; t_{il}) - f(t_{il})| \sim O(n_1^{-m}) \quad \text{as } n \to \infty.$$

The order of convergence exhibited in the latter result is 2 less than O'Cinneide's result (see Remark 3.1). The discrepancy occurs because we have assumed less restrictive conditions than O'Cinneide. The following corollary shows that, if we assume that the lower-order derivatives of f are bounded and insist that n is an integer multiple of l, then we can match O'Cinneide's order of convergence.

Corollary 3.1. *If $f \in \mathcal{PC}_l^{k+1}$, $f^{(2)}$ is bounded and n is a multiple of l, then, letting $r_0 := \min(k+1, m+3)$, we have*

$$|E_n(l, m; t_{il}) - f(t_{il})| \sim O\left(\left(n + \frac{(m+1)l}{2}\right)^{-(r_0-1)}\right) \quad \text{as } n \to \infty.$$

Proof. We see that r_0 is restricted by the lesser of $k+1$ and $m+3$. We know from the proof of Theorem 3.2 that the $k+1$ limit arises when the limited differentiability of f prevents further integration by parts. Our task here is to find the mechanism behind the $m+3$ limit. We assume that $k \geq m+2$, which means that we can write (3.14) as

$$\Delta\tilde{E}_n(l, m; t_{il}) = (-1)^{\lfloor 3(m+1)/2 \rfloor} \frac{2}{\pi n_1^{m+1}} \int_0^{2\pi} f_c^{(m+1)}(u)\phi_{m+1}(n_1 u)\, \mathrm{d}u. \tag{3.17}$$

Suppose that we subdivide $[0, 2\pi]$ into subintervals throughout each of which $f_c^{(m+1)}$ is continuous. By virtue of our assumption about where f and its derivatives may possess discontinuities, the limits of these subintervals will occur at points $t'_{jl} - t_{il}$. The integral in (3.17) can then be expressed as a finite sum of integrals over these subintervals. Clearly, integration by parts on the original integral is effected by integrating by parts over each of the 'subintegrals'.

Now, if $m+1$ is odd, $\phi_{m+1}(n_1 u) = \sin(n_1 u)$ from (3.16), and then obviously the integral of $\phi_{m+1}(n_1 u)$ is $-\cos(n_1 u)$. Given that n is an integer multiple of l, it is easy to show that $\cos(n_1 u) = 0$ when $u = t'_{jl} - t_{il}$. Conversely, if $m+1$ is even, the integral of $\phi_{m+1}(n_1 u)$ is $\sin(n_1 u)$, and it follows that $\sin(n_1 u) = 0$ when $u = t'_{jl} - t_{il}$. From these arguments, we conclude that, upon integrating by parts once more in (3.17), the nonintegral terms vanish, leaving

$$\Delta\tilde{E}_n(l, m; t_{il}) = (-1)^{\lfloor 3(m+2)/2 \rfloor} \frac{2}{\pi n_1^{m+2}} \int_0^{2\pi} f_c^{(m+2)}(u)\phi_{m+2}(n_1 u)\, \mathrm{d}u. \tag{3.18}$$

By an extension of the integrability argument given in the proof of Theorem 3.2, the boundedness of $f^{(1)}$ ensures the integrability of $f_c^{(m+2)}$ in (3.18). Appealing to the boundedness of $f^{(2)}$, we apply integration by parts one more time to (3.18) to obtain that

$$|\Delta\tilde{E}_n(l, m; t_{il})| \leq \frac{C}{n_1^{m+3}}, \tag{3.19}$$

where C is a positive constant independent of n. Finally, we infer from (3.19) that

$$|E_n(l, m; t_{il}) - f(t_{il})| \sim O(n_1^{-(m+2)}) \quad \text{as } n \to \infty.$$

This completes the proof.

4. Other sequence transformations

In the previous section, we saw that Euler(l, m) summation is an effective technique for convergence acceleration of Fourier partial sums S_n of piecewise-smooth functions. But Euler(l, m) summation is by no means the only technique that will work. In this section, we give a brief overview of other sequence transformations that can accelerate convergence of slowly convergent Fourier partial sums.

Sequence transformations can be broadly classified as either linear or nonlinear (see [40] for details). We have seen that Euler summation is an example of a linear sequence transformation. Linear sequence transformations are called *Fourier space filters* in the literature on spectral methods. Vandeven [39] (see also [24]) defined a class of Fourier space filters that are accelerative for piecewise-smooth functions. He showed that, if f is piecewise C^k, then for a filter $\sigma(\theta)$ of 'order k' satisfying certain conditions, the filtered partial sum of the Fourier series

$$S_n^\sigma(t) = \sum_{j=-n}^{n} \sigma\left(\frac{j}{n}\right) c_k e^{ijt}$$

satisfies

$$|f(t) - S_n^\sigma(t)| \leq \frac{K}{d(t)^{k-1} n^{k-1}}, \tag{4.1}$$

where $d(t)$ is the distance of t from the nearest discontinuity and K is a constant. Unfortunately, these filters are unable to achieve uniform convergence over the range of t; there is a rapid deterioration of accuracy as t approaches a discontinuity, which is suggested by the presence of the factor $d(t)$ in (4.1). Recall (see Remark 3.2) that Euler(l, m) summation exhibits a similar nonuniformity of convergence.

The classical Lanczos and raised-cosine filters belong to Vandeven's class of filters, with orders 1 and 2 respectively. Vandeven [39] himself introduced a filter—which we shall refer to as the Vandeven–Daubechies filter—whose order can be made arbitrarily large. The Vandeven–Daubechies filter is optimal in the sense that it minimizes the constant K in (4.1). While classical Euler summation and Euler(l, m) summation do not belong to Vandeven's class, Boyd [6] derived the interesting result that classical Euler summation of order m and the Vandeven–Daubechies filter of order $(m + 2)/2$ are asymptotically equivalent in m.

Several nonlinear transformations have been tested with the Fourier-series inversion method, namely Wynn's ε-algorithm (see [13], [16] and [18]), the quotient-difference (q-d) algorithm (see [17] and [14]) and Levin's u-transformation (see [18]). Like linear methods, nonlinear methods also exhibit nonuniformity of convergence with respect to distance from the discontinuities (see [5] for graphical results for the ε-algorithm and u-transformation applied to the Fourier series of a sawtooth function). The ε-algorithm and the q-d algorithm have been found to work well when the inversion point is far from any discontinuities. Comparisons by Crump [13] and Honig and Hirdes [27] suggest that the ε-algorithm gives faster convergence than classical Euler summation. However, the ε- and q-d algorithms suffer the drawback of numerical instability under certain circumstances; for instance, rounding errors can completely dominate when high-order terms are computed. In contrast, classical Euler summation and Euler(l, m) summation are numerically very stable (see [35, pp. 328–329]).

Before closing this section, we mention that there are other techniques for recovering point values of a piecewise-smooth function besides sequence transformations. In particular, there are the recent approaches of Gottlieb and Shu [24] and Eckhoff [20] that can, in theory, recover values close to the discontinuities. Discussion of these techniques is postponed until Section 7.

5. Overcoming discontinuities at arbitrary locations

In Section 2, we verified that Euler(l, m) summation is accelerative for Fourier series of piecewise-smooth functions with discontinuities at the special points t'_{il}. In this section, we consider the more general problem of dealing with functions with discontinuities at arbitrary

locations. Except for [1], this problem has received little attention in the literature on numerical transform inversion.

Abate and Whitt [1, Section 14] highlighted the limitations of the Fourier-series family of inversion techniques when the inverse function has discontinuities at arbitrary locations. They pointed out that, for some simple cases of probability distributions with atoms, the atoms can be removed before the inversion step to avoid difficulties. Unfortunately, it is not always possible to remove the discontinuities. In such cases, Abate and Whitt suggested the use of *convolution smoothing*. Convolution smoothing refers to Fourier space filtering with a 'smooth' filter function or window. Abate and Whitt give examples using filters based on Gaussian and Hamming windows and demonstrate that moderate accuracy can be achieved away from the discontinuities (see Sections 10 and 14 of [1]). Convolution smoothing is essentially equivalent to filtering with a filter of the Vandeven class (see [39] and [24]). The Hamming filter corresponds to a raised-cosine filter, which is a second-order Vandeven-class filter, and the Gaussian window corresponds to an exponential filter of order 2, which is nearly a second-order Vandeven-class filter if the variance is suitably chosen.

In this section, we devise a new method that exploits properties of Euler(l, m) summation revealed in Section 3. Our method is based on a new variant of Euler summation that creates a *generalized* product-smoothing framework. We introduce and analyse our method in Section 5.1, and discuss parameter selection in Section 5.2. In our method, we assume that the locations of the discontinuities are known in advance (we comment on the validity of this assumption in Section 6).

Before moving on to discuss our method, we briefly mention an alternate approach that simply uses Euler(l, m) summation. The idea is to select l and t_{il} so that each discontinuity is smoothed by a product-smoothing point from the set $\{t'_{il}\}$. A little reasoning determines that this approach reduces to an integer linear programming problem in $D + 1$ unknowns, where D is the number of discontinuities (not counting any discontinuity at zero which is smoothed automatically). Unfortunately, solving this problem is not straightforward in general, and the complexity grows rapidly with the number of discontinuities.

5.1. A variant of Euler summation for generalized product smoothing

In Section 3, we found that Euler(l, m) summation results in product smoothing at the points t'_{il}. Now we introduce a new variant of Euler summation that yields generalized product smoothing. We call this variant Euler$(L, m, \pm y)$ summation. In Euler$(L, m, \pm y)$ summation, the parameter m serves the same role as m in Euler(l, m) summation, while the real parameter y and integer parameter L together dictate the locations of the smoothing points. As we shall see, Euler$(L, m, \pm y)$ summation is actually a composite of two successive summation operations using different signs of the parameter y. We will use the terms Euler(L, m, y) summation and Euler$(L, m, -y)$ summation to denote these component operations.

Let $\{a_n\}$ be a convergent sequence of complex numbers. We define the Euler(L, m, y) transformation of $\{a_n\}$ to be the sequence

$$b_n = \frac{1}{d_m(y)} \sum_{j=0}^{m} \binom{m}{j} \mathrm{e}^{\mathrm{i}(m-j)y} a_{n+jL},$$

where

$$d_m(y) = \sum_{j=0}^{m} \binom{m}{j} \mathrm{e}^{\mathrm{i}(m-j)y} = 2^m \mathrm{e}^{\mathrm{i}ym/2} \cos^m\left(\frac{y}{2}\right).$$

Similarly, we define the Euler$(L, m, -y)$ transformation of $\{a_n\}$ to be the sequence

$$b'_n = \frac{1}{d_m(-y)} \sum_{j=0}^{m} \binom{m}{j} \mathrm{e}^{-\mathrm{i}(m-j)y} a_{n+jL}.$$

By the Toeplitz theorem concerning regularity of a linear sequence transformation (see [25, p. 43] or [40, p. 27]), it can be readily verified that the Euler(L, m, y) and Euler$(L, m, -y)$ transformations are regular.

Euler(L, m, y) summation applied to the partial sums (3.6) yields that

$$\begin{aligned}
T_n &:= \frac{1}{d_m(y)} \sum_{j=0}^{m} \binom{m}{j} \mathrm{e}^{\mathrm{i}(m-j)y} E_{n+jL}(l, m; t) \\
&= \frac{1}{2\pi d_m(y)} \sum_{j=0}^{m} \binom{m}{j} \mathrm{e}^{\mathrm{i}(m-j)y} \int_0^{2\pi} f(u+t) \frac{\cos^m(lu/2) \sin(n + jL + (1+lm)/2)u}{\sin u/2} \,\mathrm{d}u \\
&= \frac{1}{4\mathrm{i}\pi d_m(y)} \int_0^{2\pi} f(u+t) \frac{\cos^m(lu/2)}{\sin u/2} \Bigg[\mathrm{e}^{\mathrm{i}(n+(1+lm)/2)u} \sum_{j=0}^{m} \binom{m}{j} \mathrm{e}^{\mathrm{i}(m-j)y} \mathrm{e}^{\mathrm{i}jLu} \\
&\qquad - \mathrm{e}^{-\mathrm{i}(n+(1+lm)/2)u} \sum_{j=0}^{m} \binom{m}{j} \mathrm{e}^{\mathrm{i}(m-j)y} \mathrm{e}^{-\mathrm{i}jLu} \Bigg] \mathrm{d}u \\
&= \frac{1}{4\mathrm{i}\pi d_m(y)} \int_0^{2\pi} f(u+t) \frac{\cos^m(lu/2)}{\sin u/2} [\mathrm{e}^{\mathrm{i}(n+(1+lm)/2)u} (\mathrm{e}^{\mathrm{i}y} + \mathrm{e}^{\mathrm{i}Lu})^m \\
&\qquad - \mathrm{e}^{-\mathrm{i}(n+(1+lm)/2)u} (\mathrm{e}^{\mathrm{i}y} + \mathrm{e}^{-\mathrm{i}Lu})^m] \,\mathrm{d}u. \qquad (5.1)
\end{aligned}$$

Euler$(L, m, -y)$ summation applied to (5.1) results in

$$\begin{aligned}
T'_n &:= \frac{1}{d_m(-y)} \sum_{j=0}^{m} \binom{m}{j} \mathrm{e}^{-\mathrm{i}(m-j)y} T_{n+jL} \\
&= \frac{1}{4\mathrm{i}\pi d_m(y) d_m(-y)} \sum_{j=0}^{m} \binom{m}{j} \mathrm{e}^{-\mathrm{i}(m-j)y} \int_0^{2\pi} f(u+t) \frac{\cos^m(lu/2)}{\sin u/2} \\
&\qquad \times [\mathrm{e}^{\mathrm{i}(n+jL+(1+lm)/2)u} (\mathrm{e}^{\mathrm{i}y} + \mathrm{e}^{\mathrm{i}Lu})^m - \mathrm{e}^{-\mathrm{i}(n+jL+(1+lm)/2)u} (\mathrm{e}^{\mathrm{i}y} + \mathrm{e}^{-\mathrm{i}Lu})^m] \,\mathrm{d}u \\
&= \frac{1}{2^{2m+2}\mathrm{i}\pi \cos^{2m}(y/2)} \int_0^{2\pi} f(u+t) \frac{\cos^m(lu/2)}{\sin u2} \\
&\qquad \times [\mathrm{e}^{\mathrm{i}(n+(1+lm)/2)u} (\mathrm{e}^{\mathrm{i}y} + \mathrm{e}^{\mathrm{i}Lu})^m (\mathrm{e}^{-\mathrm{i}y} + \mathrm{e}^{\mathrm{i}Lu})^m \\
&\qquad - \mathrm{e}^{-\mathrm{i}(n+(1+lm)/2)u} (\mathrm{e}^{\mathrm{i}y} + \mathrm{e}^{-\mathrm{i}Lu})^m (\mathrm{e}^{-\mathrm{i}y} + \mathrm{e}^{-\mathrm{i}Lu})^m] \,\mathrm{d}u \\
&= \frac{1}{2\pi \cos^{2m}(y/2)} \int_0^{2\pi} f(u+t) \\
&\qquad \times \frac{\cos^m(lu/2) \cos^m((y - Lu)/2) \cos^m((y + Lu)/2) \sin(n + Lm + (1+lm)/2)u}{\sin u/2} \,\mathrm{d}u. \qquad (5.2)
\end{aligned}$$

We now consider the effect of D successive applications of Euler$(L, m, \pm y)$ summation to (3.6) with different L and y at each step. Specifically, we apply Euler$(L_1, m, \pm y_1)$ summation

to the sequence (3.6), and then apply Euler$(L_2, m, \pm y_2)$ summation to the resulting sequence, and so on, until the final step in which we apply Euler$(L_D, m, \pm y_D)$ summation. We call the composite operation Euler$(\boldsymbol{L}, m, \pm \boldsymbol{y})$ summation, where $\boldsymbol{L} := (l, L_1, L_2, \ldots, L_D)$ and $\boldsymbol{y} := (y_1, y_2, \ldots, y_D)$, and denote the resulting sequence by $E_n(\boldsymbol{L}, m, \boldsymbol{y}; t)$. Our motivation here is to construct a generalized product-smoothing framework that can smooth D distinct discontinuities located at arbitrary points within the interval $[0, 2\pi]$.

Applying similar arguments to those used to derive (5.1) and (5.2), we find that

$$E_n(\boldsymbol{L}, m, \boldsymbol{y}; t) = \frac{1}{2\pi \prod_{p=1}^{D} \cos^{2m}(y_p/2)} \int_0^{2\pi} f(u+t) \frac{\cos^m(lu/2)}{\sin u/2} \times \left(\prod_{p=1}^{D} \cos^m\left(\frac{y_p - L_p u}{2}\right) \cos^m\left(\frac{y_p + L_p u}{2}\right)\right) \times \sin\left(n + \frac{1+lm}{2} + m\sum_{p=1}^{D} L_p\right) u \, \mathrm{d}u. \tag{5.3}$$

Now consider the first difference, $\Delta E_n(\boldsymbol{L}, m, \boldsymbol{y}; t)$. From (5.3) we obtain that

$$\Delta E_n(\boldsymbol{L}, m, \boldsymbol{y}; t) = \frac{1}{\pi \prod_{p=1}^{D} \cos^{2m}(y_p/2)} \int_0^{2\pi} f(u+t) \cos^m\left(\frac{lu}{2}\right) \times \left(\prod_{p=1}^{D} \cos^m\left(\frac{y_p - L_p u}{2}\right) \cos^m\left(\frac{y_p + L_p u}{2}\right)\right) \times \cos\left(n + \frac{lm}{2} + m\sum_{p=1}^{D} L_p\right) u \, \mathrm{d}u. \tag{5.4}$$

We consider (5.3) and (5.4) evaluated at $t = t_{il}$. We infer from (5.4) that, in addition to product smoothing of f at the argument values t'_{il} due to the factor $\cos^m(lu/2)$, $E_n(\boldsymbol{L}, m, \boldsymbol{y}; t_{il})$ features product smoothing of f at other points due to the factors $\cos^m((y_p - L_p u)/2)$ and $\cos^m((y_p + L_p u)/2)$. Specifically, these factors induce product smoothing of f at the argument values

$$\bar{t}_{jL_p} = \frac{(2j-1)\pi + y_p}{L_p} + t_{il}, \qquad p = 1, 2, \ldots, D, \ j \in \mathbb{Z}, \tag{5.5}$$

and

$$\underline{t}_{jL_p} = \frac{(2j-1)\pi - y_p}{L_p} + t_{il}, \qquad p = 1, 2, \ldots, D, \ j \in \mathbb{Z}. \tag{5.6}$$

Next, we state the main result of this section. It applies to the space of functions that have $k+1$ piecewise-continuous derivatives. The function f and its derivatives are permitted discontinuities at the points t'_{il}, $\bar{t}_{jL_p}$ and $\underline{t}_{jL_p}$ and these discontinuities may be of infinite type. We denote this class of functions by $\mathcal{PC}^{k+1}_{\boldsymbol{L}}$.

Theorem 5.1. *For $f \in \mathcal{P}\mathcal{C}_{\boldsymbol{L}}^{k+1}$ and $r_1 := \min(k+1, m)$, the approximation error incurred by $E_n(\boldsymbol{L}, m, \boldsymbol{y}; t_{il})$ satisfies the bound*

$$|E_n(\boldsymbol{L}, m, \boldsymbol{y}; t_{il}) - f(t_{il})| \leq \frac{\|f_{\mathrm{c}}^{(r_1)}\|_1}{\pi|\psi|(r_1-1)(n+ml/2+m\sum_{p=1}^{D} L_p)^{r_1-1}},$$

where

$$f_{\mathrm{c}}(u) := f(u+t_{il})\cos^m\left(\frac{lu}{2}\right)\left(\prod_{p=1}^{D}\cos^m\left(\frac{y_p - L_p u}{2}\right)\cos^m\left(\frac{y_p + L_p u}{2}\right)\right)$$

and

$$\psi := \prod_{p=1}^{D}\cos^{2m}\left(\frac{y_p}{2}\right).$$

Proof. The proof outlined here is similar to that of Theorem 3.2. Let

$$n_2 := n + \frac{lm}{2} + m\sum_{p=1}^{D} L_p.$$

The equation (5.4) evaluated at $t = t_{il}$ can be written as

$$\Delta E_n(\boldsymbol{L}, m, \boldsymbol{y}; t_{il}) = \frac{1}{\pi\psi}\int_0^{2\pi} f_{\mathrm{c}}(u)\cos(n_2 u)\,\mathrm{d}u.$$

We define

$$\chi(u) := \cos^m\left(\frac{lu}{2}\right)\left(\prod_{p=1}^{D}\cos^m\left(\frac{y_p - L_p u}{2}\right)\cos^m\left(\frac{y_p + L_p u}{2}\right)\right).$$

By definition, $f(u+t_{il})$ and its derivatives have possible discontinuities when $u + t_{il} = \tau$ and τ equals t'_{jl}, $\bar{t}_{jL_p}$ or $\underline{t}_{jL_p}$, where these points are defined in (3.9), (5.5) and (5.6) respectively. However, since χ has zeros of order m at the points $\tau - t_{il}$, we conclude that $f_{\mathrm{c}} \in \mathrm{C}^{\gamma_1}$, where $\gamma_1 = \min(k+1, m-1)$. The continuity of f_{c} and its derivatives ensures that, when we iteratively integrate (3.13) by parts r_1 times, all leading terms vanish and we are left with

$$\Delta E_n(\boldsymbol{L}, m, \boldsymbol{y}; t_{il}) = (-1)^{\lfloor 3r_1/2\rfloor}\frac{1}{\pi\psi n_2^{r_1}}\int_0^{2\pi} f_{\mathrm{c}}^{(r_1)}(u)\phi_{r_1}(n_2 u)\,\mathrm{d}u, \tag{5.7}$$

where ϕ_{r_1} is given by (3.16).

From (5.7) we obtain that

$$|\Delta E_n(\boldsymbol{L}, m, \boldsymbol{y}; t_{il})| \leq \frac{\|f_{\mathrm{c}}^{(r_1)}\|_1}{\pi|\psi|n_2^{r_1}}.$$

The bound on the approximation error can then be determined as

$$\begin{aligned}|E_n(\boldsymbol{L}, m, \boldsymbol{y}; t_{il}) - f(t_{il})| &\leq \sum_{j=n+1}^{\infty}|\Delta E_n(\boldsymbol{L}, m, \boldsymbol{y}; t_{il})| \\ &\leq \frac{\|f_{\mathrm{c}}^{(r_1)}\|_1}{\pi|\psi|(r_1-1)n_2^{r_1-1}}.\end{aligned}$$

This completes the proof.

5.2. Parameter selection for Euler($\boldsymbol{L}, m, \pm\boldsymbol{y}$) summation

The parameter set of Euler($\boldsymbol{L}, m, \pm\boldsymbol{y}$) summation consists of those parameters specific to it, namely $y_1, y_2, \ldots, y_D$ and $L_1, L_2, \ldots, L_D$, as well as those inherited from Euler(l, m) summation, namely l, m and n. Parameter-selection strategies for l, m and n in Euler(l, m) summation are discussed at length in [1], [3] and [35]. The theory of Section 3 and our numerical experience support applying the same strategies for l, m and n in Euler($\boldsymbol{L}, m, \pm\boldsymbol{y}$). In this section, we derive rules for choosing values for the parameters $y_1, y_2, \ldots, y_D$ and $L_1, L_2, \ldots, L_D$.

First, let us assume that f has only one discontinuity internal to $[0, 2\pi]$ and that it occurs at the point τ. Since there is only one discontinuity, we use Euler($\boldsymbol{L}, m, \pm\boldsymbol{y}$) summation with $\boldsymbol{L} = (l, L)$ and $\boldsymbol{y} = y$. The goal is to choose L and y so that one of the smoothing points $\bar{t}_{jL}$ or $\underline{t}_{jL}$ falls on τ. A possible strategy is to fix L (to be equal to l, say) and adjust y so that one of the smoothing points is placed at τ. The equations (5.5) and (5.6) show that, by varying y and holding L fixed, we have complete control of $\bar{t}_{jL}$ and $\underline{t}_{jL}$. This strategy, however, will fail for general τ due to rounding error. To see this, observe from (5.3) that $E_n(\boldsymbol{L}, m, \boldsymbol{y}; t)$ contains a prefactor $1/\cos^{2m}(y/2)$. We denote this quantity by

$$\eta := \frac{1}{\cos^{2m}(y/2)}. \tag{5.8}$$

If $\cos(y/2)$ is allowed to become too small, η will be large, causing a large magnification of rounding error. Clearly, the worst case occurs when $y = (2j-1)\pi$ for some integer j. Chen and O'Cinneide [10] encountered a similar rounding-error problem for their generalized Euler summation algorithm.

To avoid the rounding-error problem, we must not allow y to deviate far from an integer multiple of 2π. The following approach is proposed: adjust L so that $\bar{t}_{jL}$ (or $\underline{t}_{jL}$) is equal to τ, while satisfying the constraint that y is close to an integer multiple of 2π. Note that, in general, it is not possible to make y exactly an integer multiple of 2π because of the integral nature of L. We now describe an algorithm to implement our approach.

We define the ratio

$$\theta := \frac{\tau}{t_{il}}. \tag{5.9}$$

Our goal is to choose the parameters L and y so that one of the points $\bar{t}_{jL}$ or $\underline{t}_{jL}$ is equal to τ. Suppose that we make $\bar{t}_{1L} = \tau$. (Similar arguments to those presented below apply if we make $\underline{t}_{1L} = \tau$.) From (5.5) we have

$$y = Lt_{il}(\theta - 1) - \pi. \tag{5.10}$$

We assume, as is usual in Euler(l, m) summation, that $t_{1l} = \pi/l$. Since we have $0 < \tau < 2\pi$, θ is in the range $0 < \theta < 2l$. Our rules for selecting L and y are as follows:

1. If $0 < \theta < 1$, select L so that $y \approx -2\pi$. This means assigning
$$L = \max\left(\left\langle \frac{l}{1-\theta} \right\rangle, 1\right). \tag{5.11}$$
2. If $1 < \theta < 2l$, select L so that $y \approx 2(j-1)\pi$ for j a positive integer. In other words, we assign
$$L = \max\left(\left\langle \frac{l(2j-1)}{\theta - 1} \right\rangle, 1\right). \tag{5.12}$$

Here, $\langle x \rangle$ denotes the integer nearest to x.

We compute L from (5.11) or (5.12), using $j = 1$ as a starting point, and then substitute that value into (5.10) to obtain the true value of y. For L obtained from (5.12), the resulting prefactor η given by (5.8) can occasionally be large enough to raise concerns about rounding error. To avoid problems, if η exceeds some predefined threshold, we increment j in (5.12) by 1 and re-compute L, y and η. We repeat until we find an η less than the threshold. Through numerical experiments, the author has found that 100 is a suitably conservative threshold value. For $l = 1$, the condition $\eta < 100$ is satisfied everywhere with $j = 1$; for $l = 2$, $\eta < 100$ is satisfied everywhere with a combination of $j = 1$ and $j = 2$.

The numerical experience has been that, provided the inversion point is not too close to a discontinuity, our selection rules for L and y based on (5.11), (5.12) and (5.10) control the rounding error well. These rules cause L to tend to l when θ tends to 0 or $2\pi/t_{il}$. On the other hand, when θ approaches 1 from above or below, $L \to \infty$. In other words, the computational cost of the algorithm increases without bound as we move the inversion point closer to a discontinuity. Even if we do not place restrictions on the computational budget, Euler($\boldsymbol{L}, m, \pm\boldsymbol{y}$) summation will ultimately fail when t_{1l} is too close to a discontinuity due to the rounding-error problems associated with summing a large number of terms.

The inability to invert close to a discontinuity is clearly a limitation. However, we do not consider it to be a serious problem for probability applications since, as Abate and Whitt [1] point out, 'we rarely need to know the CDF precisely in the neighbourhood of a jump'. Furthermore, theory and numerical experiments show (see Section 6) that with Euler($\boldsymbol{L}, m, \pm\boldsymbol{y}$) summation we can typically invert to about $\pm 2\%$ of the location of a discontinuity while requiring only about 1000 terms of the Fourier series, a value we consider to be moderate in terms of the computation required. However, the fact remains that, if we truly wish to invert at or in the immediate vicinity of a discontinuity, another method must be found. We briefly discuss possible approaches in Section 7.

In the general case when f has D discontinuities internal to $[0, 2\pi]$, the idea is to apply Euler($\boldsymbol{L}, m, \pm\boldsymbol{y}$) summation with $\boldsymbol{L} = (l, L_1, L_2, \ldots, L_D)$ and $\boldsymbol{y} = (y_1, y_2, \ldots, y_D)$. For $p = 1, 2, \ldots, D$, the parameters L_p and y_p are selected to smooth the pth discontinuity in accordance with (5.11), (5.12) and (5.10).

6. Algorithm EULER-GPS

In this section, we describe and test a Fourier-series inversion algorithm for piecewise-smooth inverse functions, which is based on the findings of Section 5. We call this algorithm EULER-GPS, where the acronym GPS stands for generalized product smoothing. EULER-GPS is characterized by the use of Euler($\boldsymbol{L}, m, \pm\boldsymbol{y}$) summation to accelerate convergence of the infinite series in (2.11). The parameters of EULER-GPS are selected according to the rules described in Section 5.2.

A premise of EULER-GPS is that the locations of the discontinuities are known. In many probability applications, the locations of the discontinuities can be ascertained after a little analysis. For instance, if the transform to be inverted represents a convolution of known discontinuous distributions, then the locations of the discontinuities in the convolution distribution are related to the locations of the discontinuities in the component distributions via the convolution operation. It is also possible to estimate the locations of jump and contact discontinuities via analysis in the Fourier domain (see [19] and [22]).

The exponential damping (2.2) of g that is inherent in EULER and EULER-GPS tends to reduce the impact of discontinuities. Exponential damping reduces the absolute variation in the function values around a point of discontinuity, leading to a more rapidly converging

Fourier series. For discontinuities of g lying to the right of the inversion point, the damping is greater and, thus, so too is the benefit. In fact, the author's numerical experience is that, provided an appropriate level of damping is applied, discontinuities of g located to the right of the point $t = 2\pi/h$ (with h given by (2.9)) cause minimal impediment to the rate of convergence. As a consequence, when applying EULER-GPS, it is only necessary to smooth the nonsmooth points that lie in the interval $[0, 2\pi/h]$.

Before proceeding to the numerical examples, we define some quantities that we will need in order to assess the performance of EULER-GPS. First, we introduce the notation $L_p(t) := L_p$ and $y_p(t) := y_p$ to reflect the dependence of these parameters on the inversion point t. Next we state an expression for the total number of transform evaluations $N(t)$ required by EULER-GPS. When there are D discontinuities, $N(t)$ is given by

$$N(t) = (n' + 1 + m)l + 2m \sum_{p=1}^{D} L_p(t), \tag{6.1}$$

where n' is related to n via (3.8).

Another quantity of interest is the *magnification factor* $\eta(t)$, defined as

$$\eta(t) := \max_p \left(\left| \cos^{-m} \left(\frac{y_p(t)}{2} \right) \right| \right).$$

We will illustrate the magnification factor for some of our examples to confirm that our algorithm controls this source of rounding error.

6.1. Numerical examples

In this section, we present numerical examples to illustrate the performance of EULER-GPS. For comparison, we also give results for EULER. We use simple examples for which the exact inverse-function values are known. All computations were performed in double-precision arithmetic.

6.1.1. *A unit point mass.* Our first example is the cumulative distribution function (CDF) of a unit point mass situated at $t = 5$. The CDF therefore has a jump discontinuity of unit magnitude at $t = 5$.

EULER and EULER-GPS were run with the parameter selections $l = 1$, $A = 22$ and $m = 11$. For EULER, we set $n' = 988$ so that the total number of transform evaluations was $(n' + 1 + m)l = 1000$. For EULER-GPS, we set $n' = 50$ and the total number of transform evaluations $N(t)$ was limited to a maximum of 1000 to provide a fair comparison with EULER.

Figure 1 displays the absolute errors for EULER and EULER-GPS. The total number of transform evaluations $N(t)$ for EULER-GPS is plotted in Figure 2 along with the magnification factor $\eta(t)$.

We see from Figure 1 that EULER-GPS dramatically accelerates convergence. (Note that the absolute error for EULER-GPS appears to be constant for $t > 5$ because it is dominated by aliasing error, which is constant in this region; re-running with $A = 30$ reduced aliasing error sufficiently so that the structure of noise fluctuations from rounding and truncation errors was revealed.) In contrast, the error graph for EULER reveals both a slow rate of convergence and large oscillations. The greater accuracy of EULER in the extreme left and extreme right portions of the graph deserves comment. As explained previously, when t is sufficiently far to the left of the discontinuity, exponential damping helps to mitigate the effect of the discontinuity. For $t < 2.5$, the discontinuity is outside the $2\pi/h$ period, and hence has negligible effect. Now, if

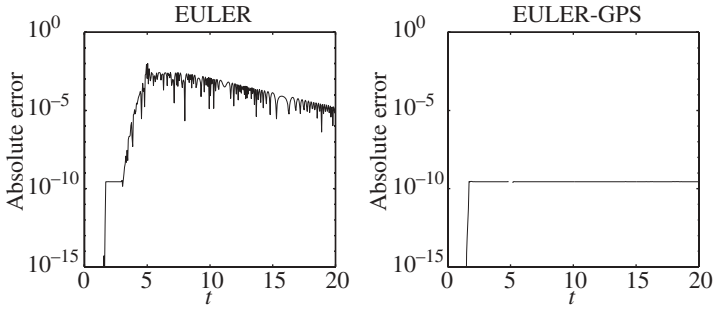

FIGURE 1: Comparison of absolute errors of EULER and EULER-GPS for a unit point mass.

we consider the region to the right of the discontinuity, we see that the error graph for EULER displays a decreasing trend as t moves further from the discontinuity. The explanation for this is that, in relation to the $2\pi/h$ period, the angular separation of the discontinuity from zero decreases with increasing t, and therefore the product smoothing at zero has an increasing smoothing influence on the discontinuity.

In a small neighbourhood of the discontinuity, the restriction $N(t) < 1000$ is violated, so we do not plot results for EULER-GPS there. We refer to this as the *large-N neighbourhood* associated with the discontinuity. This neighbourhood is found to be approximately (4.88, 5.12). Denoting the location of the discontinuity by t_{d}, we can re-express the size of the large-N neighbourhood in terms of the ratio $\theta = t_{\mathrm{d}}/t$ (which is equivalent to (5.9)), giving $\theta \in (0.98, 1.02)$. The same result can be obtained analytically using (5.11), (5.12) and (6.1). If the upper limit on $N(t)$ is relaxed to 10 000, then the large-N neighbourhood is reduced to approximately (0.998, 1.002), but experimentation shows that the absolute error increases to about 10^{-7} at the interval boundaries. The loss in accuracy is due to the rounding error incurred by summing the larger number of terms.

If t is such that we can find an L to make y an exact integer multiple of 2π, then the points $\bar{t}_{jL}$ and $\underline{t}_{jL}$ will coincide. The result is product smoothing of order $2m$. It may then be possible to reduce m (for the Euler$(L, m, \pm y)$ summation iteration) by a half without significantly undermining accuracy. Even when y is not an exact integer multiple of 2π, $\underline{t}_{jL}$ will not be too far from $\bar{t}_{jL}$ and it is plausible that the nulling effect at $\underline{t}_{jL}$ will still be felt at $\bar{t}_{jL}$. To test this hypothesis, EULER-GPS was run on the point mass example with $m = 5$ for Euler$(L, m, \pm y)$ summation (we maintained $m = 11$ for Euler(l, m) summation). The result was a reduction in accuracy near the discontinuity to about 10^{-5}, plus some slight reduction at a few other points. There was also a reduction in the size of the large-N neighbourhood, since a smaller m permits a larger maximum value of L (see (6.1)). These results suggest that it is better not to reduce m.

Figure 2 shows that the magnification factor $\eta(t)$ is of modest size. For t greater than that shown in the graph, $\eta(t)$ continues to decrease monotonically.

6.1.2. *A sequence of point masses.* Now we consider the CDF of a sequence of four point masses to demonstrate how EULER-GPS copes with multiple discontinuities. The point masses are located at 4.8, 5, 6 and 15 and have magnitudes 0.2, 0.5, 0.1 and 0.2 respectively.

The parameter selections $l = 1$, $A = 22$ and $m = 11$ were used for both EULER and EULER-GPS. We set $n' = 988$ for EULER, and $n' = 50$ and $N(t) \leq 1000$ for EULER-GPS.

Figure 3 shows the absolute errors for EULER and EULER-GPS and Figure 4 shows $N(t)$ and $\eta(t)$.

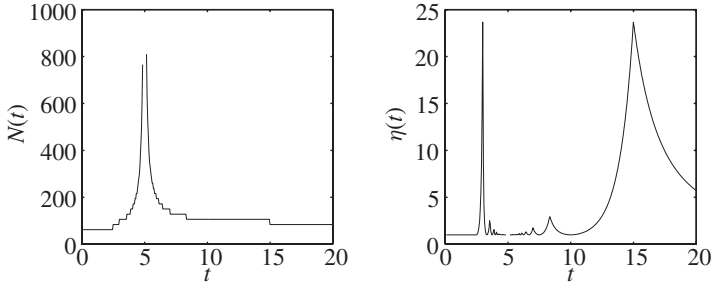

FIGURE 2: EULER-GPS performance for a unit point mass: number of transform evaluations $N(t)$ and magnification factor $\eta(t)$.

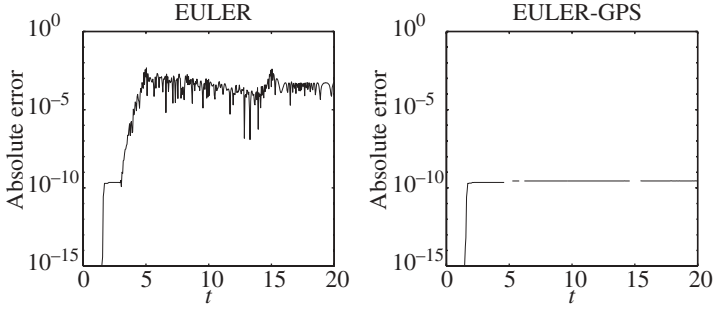

FIGURE 3: Comparison of absolute errors of EULER and EULER-GPS for point masses at $t = 4.8, 5, 6$ and 15.

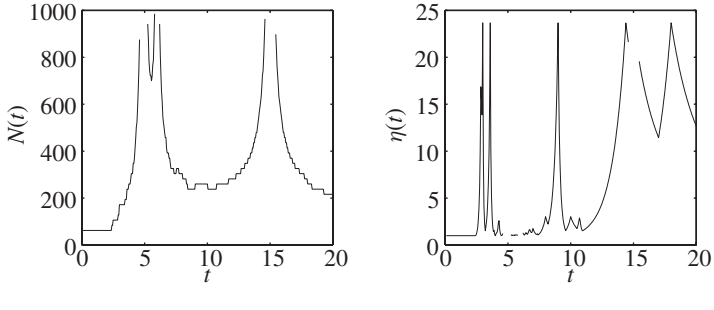

FIGURE 4: EULER-GPS performance for point masses at $t = 4.8, 5, 6$ and 15: number of transform evaluations $N(t)$ and magnification factor $\eta(t)$.

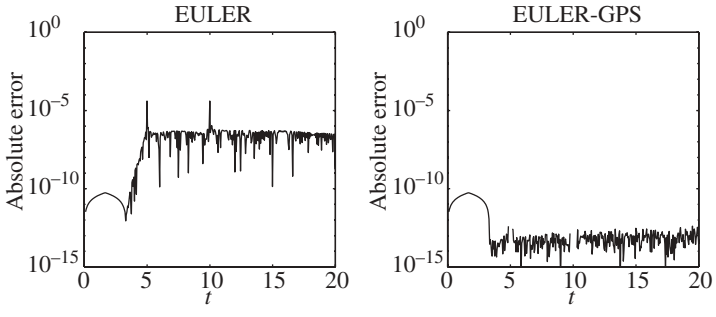

FIGURE 5: Comparison of absolute errors of EULER and EULER-GPS for a sum of two uniform(0, 5) random variables.

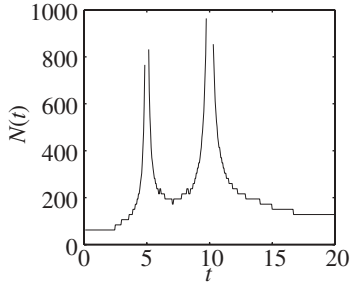

FIGURE 6: Number of transform evaluations $N(t)$ for EULER-GPS applied to a sum of two uniform(0, 5) random variables.

We observe that EULER-GPS achieves a high degree of accuracy away from the discontinuities. However, each large-N neighbourhood (measured in terms of the normalized quantity θ) is larger than that of the single point mass example because the total budget of 1000 terms must be spread across the discontinuities. Note that, because the discontinuities at $t = 4.8$ and $t = 5$ are close to each other, their large-N neighbourhoods merge.

6.1.3. *A sum of uniforms.* Here, we consider the density of a sum of two uniform(0, 5) random variables. In this case, there are no jump discontinuities, but contact discontinuities at $t = 0$, 5 and 10. The following parameter settings were used: $l = 1$, $A = 22$ and $m = 11$ for both EULER and EULER-GPS, $n' = 988$ for EULER, and $n' = 50$ and $N(t) \leq 1000$ for EULER-GPS. The absolute errors for EULER and EULER-GPS are shown in Figure 5, and $N(t)$ is plotted in Figure 6.

EULER does better here than it did for the point mass examples because the inverse function is smoother. However, it is still easily out-performed by EULER-GPS.

6.1.4. *An inverse Gaussian density.* For our last example, we consider the density of an inverse Gaussian distribution. Our aim is to demonstrate that EULER-GPS is helpful not just for overcoming discontinuities in the inverse function or its derivatives, but also for overcoming the effects of other features exhibiting rapid variation.

The density of the standard inverse Gaussian distribution is given by

$$p(t) = \left[\frac{\lambda}{2\pi t^3}\right]^{1/2} \exp\left\{-\frac{\lambda}{2\mu^2 t}(t-\mu)^2\right\}, \qquad t > 0$$

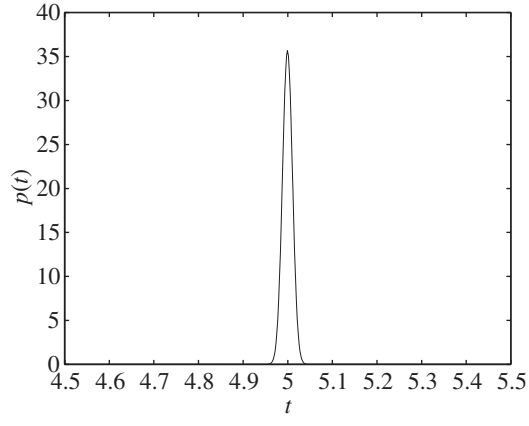

FIGURE 7: Density of an inverse Gaussian distribution with parameters $\mu = 5$ and $\lambda = 10^6$.

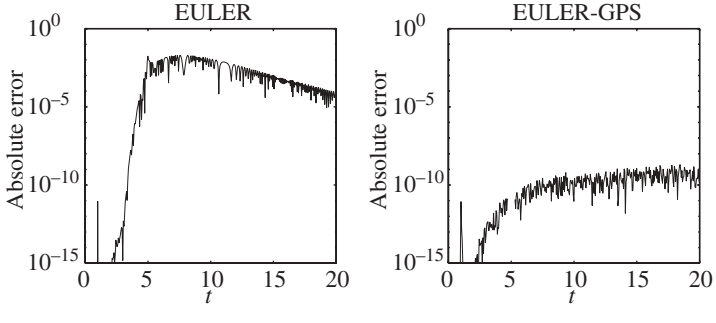

FIGURE 8: Comparison of absolute errors of EULER and EULER-GPS for the density of an inverse Gaussian distribution with parameters $\mu = 5$ and $\lambda = 10^6$.

(see [30, p. 261]). The mean is equal to μ. The density function has bounded derivatives of all orders for $t > 0$.

The Laplace transform of the inverse Gaussian distribution is

$$\hat{p}(s) = \exp\left[\frac{\lambda}{\mu}\left\{1 - \left(1 + \frac{2\mu^2 s}{\lambda}\right)^{1/2}\right\}\right]$$

(see [30, p. 262]). As λ is made large, the density becomes increasingly concentrated around $t = \mu$, giving rise to steep profiles on either side of this point. The density for $\mu = 5$ and $\lambda = 10^6$ is shown in Figure 7. In similar fashion to a point mass, the steep profiles near $t = 5$ introduce strong 'high-frequency' components into the Fourier-series expansion.

EULER and EULER-GPS were applied to the transform of the density with $\mu = 5$ and $\lambda = 10^6$, with a single smoothing point at $t = 5$ for EULER-GPS. The following parameter settings were used: $l = 2$, $A = 29$ and $m = 11$ for both EULER and EULER-GPS, $n' = 488$ for EULER, and $n' = 50$ and $N(t) \leq 1000$ for EULER-GPS. Compared to the previous examples, a larger damping parameter A was used, coupled with a larger l, in order to combat the large peak magnitude of the density function.

In Figure 8, we plot the absolute errors for EULER and EULER-GPS and, in Figure 9, we plot $N(t)$. We see that EULER-GPS is much more accurate than EULER. The small spikes

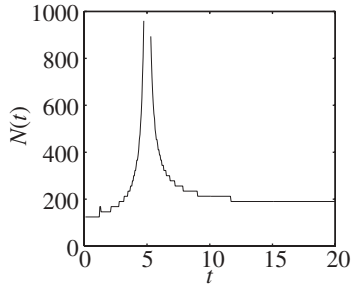

FIGURE 9: Number of transform evaluations $N(t)$ for EULER-GPS applied to the density of an inverse Gaussian distribution with parameters $\mu = 5$ and $\lambda = 10^6$.

occurring at $t = \frac{5}{3}$ in the absolute error plots are artifacts of aliasing errors caused by the spike at $t = 5$.

7. Conclusions

In this paper, we have developed a new variant of the algorithm EULER, called EULER-GPS, which is designed to cope with inverse functions with discontinuities and other regions of rapid variation. We devised a variant of Euler summation called Euler($\boldsymbol{L}$, m, $\boldsymbol{y}$) summation which forms the basis of EULER-GPS. Through numerical examples, we demonstrated that the performance of EULER-GPS is superior to that of EULER for functions containing discontinuities and steep profiles at arbitrary locations.

In our approach, we have emphasized accuracy and robustness over efficiency. This is exemplified by the fact that the algorithm EULER-GPS evaluates a new Fourier series for each t to maximize the benefit of Euler(l, m) summation. Of course, this is the same approach taken in EULER. Alternatively, it is possible to place more emphasis on efficiency by using the same Fourier series for a range of t-values; see, for instance, the generalized Euler summation algorithm of Chen and O'Cinneide [10]. It is not difficult to see that the generalized product-smoothing framework makes it possible to modify EULER-GPS to operate in this fashion.

Besides numerical transform inversion, there are other problems in applied mathematics requiring reconstruction of point values of piecewise-smooth functions from knowledge of their Fourier coefficients. An example is the use of spectral methods to solve differential equations (see [23]). We expect Euler($\boldsymbol{L}$, m, $\boldsymbol{y}$) summation to be applicable to such problems.

A limitation of EULER-GPS is that it breaks down in the neighbourhood of a discontinuity. We showed in Section 6.1 that this neighbourhood is quite small—for parameter settings $m = 11$, $n' = 50$ and $l = 1$ and the restriction $N(t) \leq 1000$, the size of the neighbourhood is about $\pm 2\%$ of the discontinuity location. If high computational cost is acceptable, the size of the neighbourhood can be reduced through the use of EULER-GPS with higher-precision arithmetic, which will permit large $N(t)$ without significant rounding error.

In recent years, several numerical schemes for overcoming the Gibbs phenomenon for Fourier series right up to the discontinuities have been proposed. They have met with varying degrees of success. The first method that we mention is the Gegenbauer polynomial approach developed by Gottlieb and Shu and their collaborators in a series of papers published in the 1990s and culminating in the review paper [24]. The idea is to expand the Fourier partial sum into a more rapidly converging series based on the Gegenbauer polynomials. The resulting series does not suffer from the Gibbs phenomenon. Theoretically, the Gegenbauer polynomial

approach can recover the point values of a piecewise-smooth function with the same accuracy as in the case of smoothness everywhere. In practice, the utility of the method is restricted (often severely) by susceptibility to rounding errors. Rounding errors occur primarily because the Gegenbauer polynomials increase sharply in magnitude as their order increases (see, for example, [21]).

Another approach aimed at improving convergence near a jump discontinuity of a piecewise-smooth function is to decompose the function into a linear combination of a smooth function and a series of step functions. An algorithm to accomplish this task has recently been proposed by Eckhoff [19], [20]. Unfortunately, there are robustness issues since the algorithm requires the solution of a system of linear equations which is potentially ill conditioned or even singular.

Though it still remains to test the algorithm EULER-GPS against these other techniques, we expect EULER-GPS to compare favourably in terms of robustness and accuracy for the case when the inversion point is not too close to a discontinuity. For inversion at or arbitrarily close to a discontinuity, a possibility worth investigating is a hybrid technique combining EULER-GPS for smoothing 'far' discontinuities with Eckhoff's method for 'near' discontinuities.

Acknowledgements

I thank W. L. Chen for providing a preprint of [10]. This work was supported by the Australian Research Council.

References

[1] Abate, J. and Whitt, W. (1992). The Fourier-series method for inverting transforms of probability distributions. *Queueing Systems* **10,** 5–88.

[2] Abate, J., Choudhury, G. L. and Whitt, W. (1996). On the Laguerre method for numerically inverting Laplace transforms. *INFORMS J. Comput.* **8,** 413–427.

[3] Abate, J., Choudhury, G. L. and Whitt, W. (2000). An introduction to numerical transform inversion and its application to probability models. In *Computational Probability*, ed. W. K. Grassman, Kluwer, Norwell, MA, pp. 257–323.

[4] Bleistein, N. and Handelsman, R. A. (1986). *Asymptotic Expansion of Integrals*, 2nd edn. Dover, New York.

[5] Boyd, J. P. (1995). A lag-averaged generalization of Euler's method for accelerating series. *Appl. Math. Comput.* **72,** 143–166.

[6] Boyd, J. P. (1996). The Erfc-Log filter and asymptotics of the Vandeven and Euler sequence accelerations. In *Proc. Third Internat. Conf. Spectral High Order Meth.*, Houston Journal of Mathematics, Houston, TX, pp. 267—276.

[7] Briggs, W. L. and Henson, V. E. (1995). *The DFT: An Owner's Manual for the Discrete Fourier Transform*. SIAM, Philadelphia, PA.

[8] Butzer, P. L. and Nessel, R. J. (1971). *Fourier Analysis and Approximation*. Birkhäuser, Basel.

[9] Carslaw, H. S. (1930). *Introduction to the Theory of Fourier's Series and Integrals*, 3rd edn. Dover, New York.

[10] Chen, W. L. and O'Cinneide, C. A. (2002). The generalized Euler summation method to invert transforms. Preprint.

[11] Choudhury, G. L., Lucantoni, D. M. and Whitt, W. (1994). Multidimensional transform inversion with applications to the transient M/G/1 queue. *Ann. Appl. Prob.* **4,** 719–740.

[12] Cooley, J. W., Lewis, P. A. W. and Welch, P. D. (1967). Application of the fast Fourier transform to computation of Fourier integrals, Fourier series, and convolution integrals. *IEEE Trans. Audio Electroacoust.* **15,** 79–84.

[13] Crump, K. S. (1976). Numerical inversion of Laplace transforms using a Fourier series approximation. *J. Assoc. Comput. Mach.* **23,** 89–96.

[14] D'Amore, L., Laccetti, G. and Murli, A. (1999). An implementation of a Fourier series method for the numerical inversion of the Laplace transform. *ACM Trans. Math. Software* **25,** 279–305.

[15] Davies, B. (2002). *Integral Transforms and Their Applications*, 3rd edn. Springer, New York.

[16] Davies, B. and Martin, B. (1979). Numerical inversion of the Laplace transform: a survey and comparison of methods. *J. Comput. Phys.* **33,** 1–32.

[17] De Hoog, F. R., Knight, J. H. and Stokes, A. N. (1982). An improved method for numerical inversion of Laplace transforms. *SIAM J. Sci. Statist. Comput.* **3,** 357–366.

[18] Duffy, D. G. (1993). On the numerical inversion of Laplace transforms: comparison of three new methods on characteristic problems from applications. *ACM Trans. Math. Software* **19,** 333–359.
[19] Eckhoff, K. S. (1995). Accurate reconstructions of functions of finite regularity from truncated Fourier series expansions. *Math. Comput.* **64,** 671–690.
[20] Eckhoff, K. S. (1998). On a high order numerical method for functions with singularities. *Math. Comput.* **67,** 1063–1087.
[21] Gelb, A. (2000). A hybrid approach to spectral reconstruction of piecewise smooth functions. *J. Sci. Comput.* **15,** 293–322.
[22] Gelb, A. and Tadmor, E. (1999). Detection of edges in spectral data. *Appl. Comput. Harmonic Anal.* **7,** 101–135.
[23] Gottlieb, D. and Orszag, S. A. (1977). *Numerical Analysis of Spectral Methods: Theory and Applications*. SIAM, Philadelphia, PA.
[24] Gottlieb, D. and Shu, C. W. (1997). On the Gibbs phenomenon and its resolution. *SIAM Rev.* **39,** 644–668.
[25] Hardy, G. H. (1963). *Divergent Series*. Oxford University Press.
[26] Hewitt, E. and Hewitt, R. E. (1979). The Gibbs–Wilbraham phenomenon: an episode in Fourier analysis. *Hist. Exact Sci.* **21,** 129–160.
[27] Honig, G. and Hirdes, U. (1984). A method for numerical inversion of Laplace transforms. *J. Comput. Appl. Math.* **10,** 113–132.
[28] Hosono, T. (1984). *Fast Inversion of Laplace Transforms by BASIC*. Kyoritsu, Tokyo (in Japanese).
[29] Jackson, D. (1930). *The Theory of Approximation*. American Mathematical Society, New York.
[30] Johnson, N. L., Kotz, S. and Balakrishnan, N. (1994). *Continuous Univariate Distributions*, Vol. 1, 2nd edn. John Wiley, New York.
[31] Johnsonbaugh, R. (1979). Summing an alternating series. *Amer. Math. Monthly* **86,** 637–648.
[32] Kao, E. P. C. (1997). *An Introduction to Stochastic Processes*. Duxbury Press, New York.
[33] Knopp, K. (1944). *Theory and Application of Infinite Series*. Blackie, London.
[34] Natanson, I. P. (1964). *Constructive Function Theory*, Vol. 1. Frederick Ungar, New York.
[35] O'Cinneide, C. A. (1997). Euler summation for Fourier series and Laplace transform inversion. *Stoch. Models* **13,** 315–337.
[36] Rolski, T., Schmidli, H., Schmidt, V. and Teugels, J. (1999). *Stochastic Processes for Insurance and Finance*. John Wiley, Chichester.
[37] Simon, R. M., Stroot, M. T. and Weiss, G. H. (1972). Numerical inversion of Laplace transforms with application to percentage labeled mitoses experiments. *Comput. Biomed. Res.* **5,** 596–607.
[38] Tijms, H. C. (2003). *A First Course in Stochastic Models*. John Wiley, Chichester.
[39] Vandeven, H. (1991). Family of spectral filters for discontinuous problems. *J. Sci. Comput.* **6,** 159–192.
[40] Wimp, J. (1981). *Sequence Transformations and Their Applications*. Academic Press, London.
[41] Zygmund, A. (1959). *Trigonometric Series*, Vol. 1. Cambridge University Press.